

- 5 Baader, W. J., Bohne, C., Cilento, G., and Dunford, H. B., Peroxidase catalyzed formation of triplet acetone and chemiluminescence from isobutyraldehyde and oxygen. *J. biol. Chem.* **260** (1985) 10217–10225.
- 6 Cadenas, E., Sies, H., Campa, A., and Cilento, G., Electronically excited states in microsomal membranes: use of chlorophyll-a as an indicator of triplet carbonyls. *Photochem. Photobiol.* **40** (1984) 661–666.
- 7 Cadenas, E., Biological chemiluminescence. *Photochem. Photobiol.* **40** (1984) 823–830.
- 8 Cilento, G., Electronic Excitation in Dark Biological Processes. Chapter 9 in Adam and Cilento¹.
- 9 Cilento, G., Generation of electronically excited triplet species in biochemical systems. *Pure appl. Chem.* **56** (1984) 1179–1190.
- 10 Förster, T. H., Mechanism of energy transfer, in: *Comprehensive Biochemistry*, vol. 22, pp. 61–81. Eds M. Florkin and E. H. Stotz. Elsevier, Amsterdam 1967.
- 11 Kenten, R. H., The oxidation of phenylacetaldehyde by plant saps. *Biochem. J.* **55** (1953) 350–360.
- 12 Nascimento, A. L. T. O., da Fonseca, L. M., Brunetti, I. L., and Cilento, G., Intracellular generation of electronically excited states. Polymorphonuclear leukocytes challenged with a precursor of triplet acetone. *Biochim. biophys. Acta* **881** (1986) 337–342.
- 13 Salim-Hanna, M., Campa, A., and Cilento, G., The α -oxidase system of young pea leaves. *Pisum sativum* as generator of electronically excited states. Excitation in the dark under natural conditions. *Photochem. Photobiol.* **45** (1987) 695–702.
- 14 Sargentini, N. J., and Smith, K. C., Much of the spontaneous mutagenesis in *Escherichia coli* is due to error-prone DNA repair: implications for spontaneous mutagenesis. *Carcinogenesis* **2** (1981) 863–872.
- 15 Schulte-Herbrüggen, T., and Cadenas, E., Electronically excited state generation during the lipoxygenase-catalyzed aerobic oxidation of arachidonates. *Photobiochem. Photobiophys.* **10** (1985) 35–51.
- 16 Slawinska, D., and Slawinski, J., Biological chemiluminescence. *Photochem. Photobiol.* **37** (1983) 709–715.
- 17 Smith, K. C., and Sargentini, N. J., Metabolically produced 'UV-like' DNA damage and its role in spontaneous mutagenesis. *Photochem. Photobiol.* **42** (1985) 801–803.
- 18 Venema, R. C., and Hug, D. H., Activation of urocanase from *Pseudonoma putida* by electronically excited triplet species. *J. biol. Chem.* **260** (1985) 12190–12193.
- 19 Villablanca, M., and Cilento, G., Enzymatic generation of electronically excited states by electron transfer. *Photochem. Photobiol.* **42** (1985) 591–597.
- 20 White, E. H., Miano, J. D., Watkins, C. J., and Breaux, E. J., Chemically produced excited states. *Ang. Chem. int. Ed. (Engl.)* **13** (1971) 229–243.

0014-4754/88/070572-05\$1.50 + 0.20/0
© Birkhäuser Verlag Basel, 1988

Physical aspects of biophotons

F.-A. Popp^a, K. H. Li^b, W. P. Mei^c, M. Galle^d and R. Neurohr^d

^aInstitute of Biophysical Cell Research, Technology Center, Opelstraße 10, D-6750 Kaiserslautern 25 (Federal Republic of Germany), ^bInstitute of Physics, The Chinese Academy of Sciences, Beijing (People's Republic of China), ^cPhysics Department, The Suzhou University, Suzhou (People's Republic of China), and ^dZoologisches Institut, Universität Saarbrücken (Federal Republic of Germany)

Summary. By comparing the theoretically expected results of photon emission from a chaotic (thermal) field and those of an ordered (fully coherent) field with the actual experimental data, one finds ample indications for the hypothesis that 'biophotons' originate from a coherent field occurring within living tissues. A direct proof may be seen in the hyperbolic relaxation dynamics of spectral delayed luminescence under ergodic conditions.

A possible mechanism has to be founded on Einstein's balance equation and, under stationary conditions, on energy conservation including a photochemical potential. It is shown that the considered equations deliver, besides the thermal equilibrium, a conditionally stable region far away from equilibrium, which can help to describe both 'biophoton emission' and biological regulation.

Key words. Photobiology; bio-communication; thermal radiation; spontaneous chemiluminescence; coherent radiation fields; exponential and hyperbolic relaxation; photochemical potential; phase transition phenomena; Bose condensation.

Introduction

Although the mechanisms of bioluminescence are still not completely known, there are ample indications that this intermittent light emission of at least 10^8 photons/s has some informational significance^{1, 20, 32}.

As well as in this more or less curious phenomenon of common 'bioluminescence' which seems to be confined to evolutionarily underdeveloped systems, photons play a fundamental role in a variety of important biological functions, namely photosynthesis^{9, 23, 33}, phototaxis and phototropism^{21, 22, 59}, photoperiodicity^{3, 7, 57}, photoreactivation^{14, 19, 30} and, last but not least, seeing^{6, 18, 36}.

More and more the interrelations between all these photobiological fields are becoming evident^{24, 25, 51, 58, 63}.

The very existence of these phenomena obliges us to give thoughtful consideration to the biological role of 'low-level luminescence' which, as the topic of this multi-author review, is discussed here from several points of view.

It is the very low intensity, ranging from a few photons/(s · cm²) up to some hundreds that provokes the prevalent opinion that this 'ultra-weak photon emission from living tissues' (PE, which is actually a quasi-continuous

photon current from all active tissues) can be only due to a spontaneous chemiluminescence without peculiar importance. This common view is based on both the 'imperfection theory'⁶⁴, according to which PE originates from metabolic aberrations, and on the fact that chemically excited states tend to fall back into thermal equilibrium by dissipation of their non-thermal overshoot energy⁵⁰. However, this point of view is too simple to be in line with the experimental results. In order to clarify the discussion, we should like to oppose to this 'chaos theory' of low-level luminescence a completely controversial 'coherence hypothesis'. The latter claims in very general terms that 'biophotons' are released from a fully coherent electromagnetic field which serves as a basis for communication in living tissues.

By comparing the expectations of these controversial hypotheses with the actual experimental results,

- 1) we may obtain indications of the real nature of the phenomenon of PE and its biological significance,
- 2) we are able to propose a mechanism that is not only able to explain the phenomenon of PE, but also links the different biological functions that may be governed by photon interactions into a common pattern.

Some recent experimental results

By way of explaining the rationale behind our approach, let us look at some examples of recent experiments, one type concerning the interaction between organisms and between cells, the other reflecting directly the coherence of the emitted signals in terms of photocount statistics. The experiments were performed with the aid of a single-photocount detector which has been described in detail in former papers (see, for instance, Popp et al.⁴¹).

Daphnia magna Straus (Crustacea, Phyllopoda) were put in darkness into water of 18 °C within the quartz cuvette of our measuring equipment⁴¹. The numbers n of daphnia were altered from 1 to 90, always selecting animals of about equal size. After each alteration the intensity of the photon emission I (counts/s) was registered. The results are displayed in figure 1. In order to compare $I(n)$ with expected intensities, we calculated a theoretical curve $I_0(n)$ by supposing highest possible self-absorption within the system, taking into account at the same time the fact that each daphnia would contribute, on the average, always the same intensity i_0 , if no distance-dependent interaction between daphnia took place. Thus we have:

$$I_0(n) = \frac{i_0 \cdot F}{f} \left(1 - \exp \left(-\frac{nf}{F} \right) \right),$$

where F is the frontal water-covered surface area of the cuvette, and f represents the highest possible cross-sectional area of a daphnia (0.04 cm²). i_0 was calculated from the linear branch of the actually measured curve. Figure 1 shows that instead of $I_0(n)$ a growth-curve-like dependence of biophoton emission $I(n)$ is observed. This result has been confirmed by similar experiments with

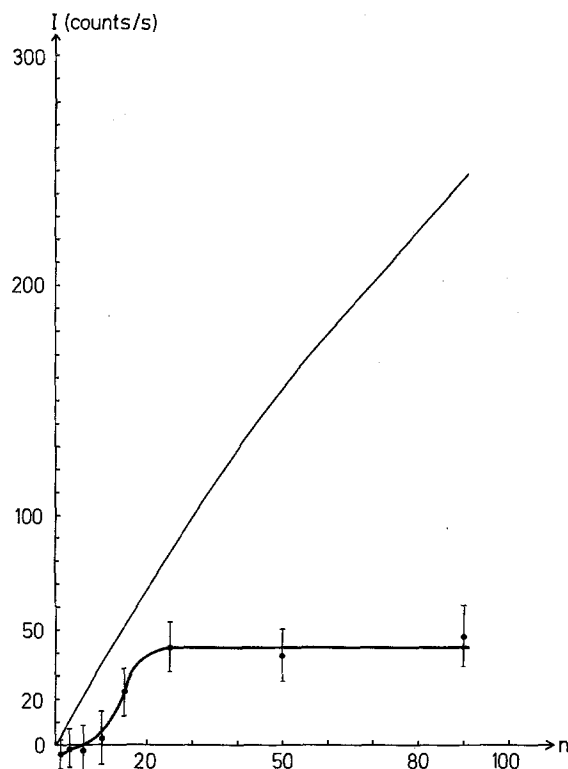


Figure 1. After insertion of n daphnia ($n = 1, 2, \dots, 90$) into the cuvette in the dark chamber, the biophoton emission (in counts/s) does not follow the expected $I_0(n)$ -curve, where a constant contribution per daphnia and the highest possible self-absorption is taken into account. Actually, a significantly different growth-curve-like biophoton intensity $I(n)$ (lower curve) is observed.

larvae of *Chironomus (tumii)* and even by investigations on moss samples which were separated in different cuvettes in the dark chamber of the equipment up to distances of 16 cm. Even then the photon intensity of the whole system was significantly different from its single parts, taking always into account a possible selfabsorption within the system under investigation. In contrast, if after excitation of one of the moss samples with light the afterglow is observed, one is obliged to introduce a *time-dependent* self-absorption of the single systems in order to describe the total emission in terms of the partial emissions and absorptions of the single separated plant structures (fig. 2).

These results indicate a resonance-like long-range interaction between the animals and the plants, correlated to their biophoton emission.

In a second experiment of this class, instead of daphnia in water, human cells in colorless medium at 37 °C were used as the subject of investigation. Since the self-emission of photons is rather weak in that case, the cell populations of different cell densities ϱ were exposed to a 3-min white-light illumination of a 150 W-tungsten lamp. The reemitted light was recorded and the decay curve of this afterglow was evaluated from 0.7 to 55 s after the end of excitation. Every sample was irradiated and measured three times consecutively; cells were stirred continuously

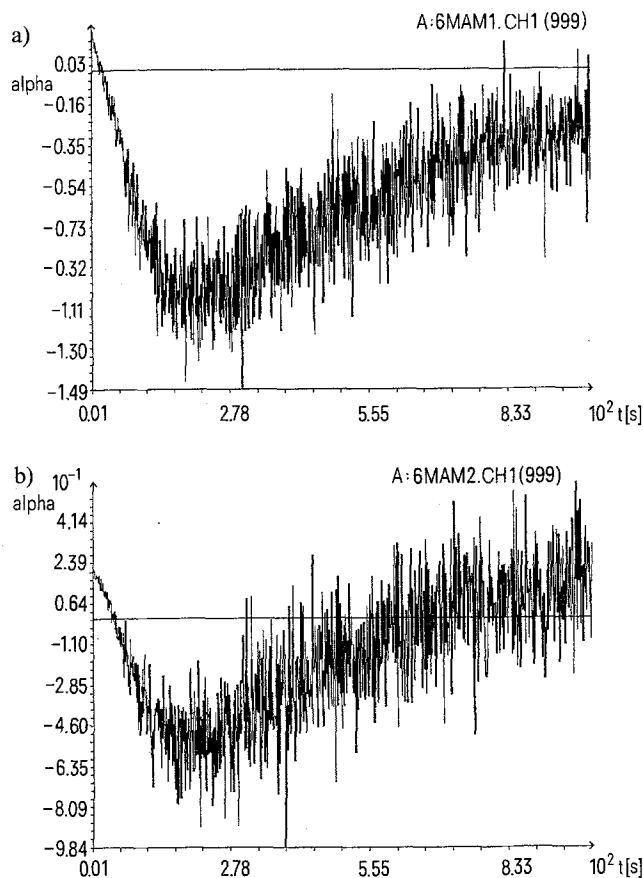


Figure 2. If one compares the photon intensity $I_1(t)$ of a moss sample I, placed in a cuvette at a distance of 20 cm from the photomultiplier, with the intensity $I_2(t)$ of just this moss sample together with a second moss sample II, placed only 4 cm from the photomultiplier away, one expects $I_2(t) = I_1(t) \cdot (1 - \alpha) + I_0$, where I_0 is the intensity of the additional second sample and α represents a constant absorption coefficient of this second sample. Figs 2a and 2b display the α -values of two consecutive experiments, calculated from the measured values $I_1(t)$, $I_2(t)$ and I_0 , where the sample I was always 0.5 s exposed to a 2000 mcd-LED-red-light-illumination before measurement. The time-dependence of α is a further indication that photons are exchanged between the systems under investigation. Sample II works here like a time-dependent *active* optical material.

in medium. In order to avoid systematic errors, the cell numbers were altered randomly. The decay curves show a much better agreement to a hyperbolic law than to an exponential one.

With a correlation coefficient of 0.99 the relaxation of I can be fitted according to the formula

$$I = A(t + t_0)^{-\frac{1}{\kappa}}$$

where A , t_0 and κ are constant, and t is the time running from 0.7 s on. While A and t_0 can be kept constant for all cell densities under investigation (ranging from 0.1 to $50 \cdot 10^6$ cells/ml), κ turns out to depend systematically on ϱ . Figure 3 displays a typical case of amnion cells (lower curve) and of a malignant form of amnion cells, namely wish cells (upper curve) which exhibits just the opposite dependence of $\kappa(\varrho)$ as the non-malignant cell population. The three measurements at the right side of figure 3 cor-

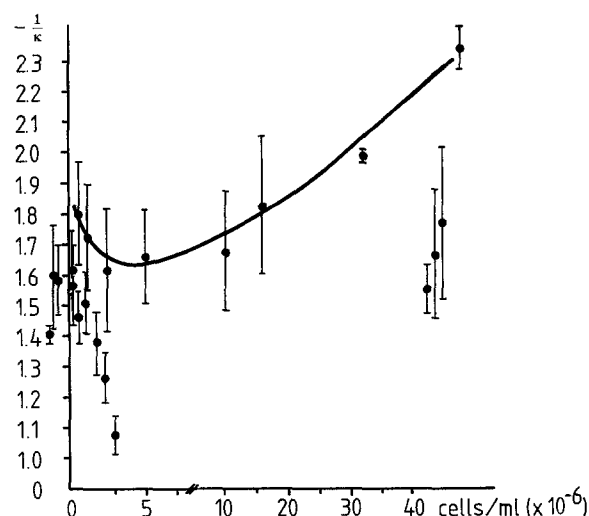


Figure 3. The decay parameter of the hyperbolic approximation $-(\text{from } I = A(t + t_0)^{-\frac{1}{\kappa}}, \text{ see text})$ that is adjusted to the relaxation dynamics of the afterglow of different cell suspensions after exposure to weak white-light illumination in dependence on the cell density. The lower curve displays the behavior of normal amnion cells. Just opposite dependence exhibit the corresponding malignant wish cells (upper curve). The three measurements at the right side of fig. 3 correspond to the nutrition medium alone.

respond to the nutrition medium alone. These diametrically opposed behaviors of normal and malignant cell populations have been found to be of quite general nature, including cell populations of plants, animals and human tissue. At the same time, they show evidence of long range interactions between cells at distances which are at least one order of magnitude higher than the size of a single cell.

In a second series of experiments we tried to establish the coherence of biophotons by photocount statistics (PCS-experiments, see Arecchi²).

As has been discussed in previous papers^{28, 41, 44, 46}, the problem of examining the coherence of biophoton emission is the unknown number M of the degrees of freedom. M increases with the number of modes under examination as well as with the sampling time Δt within which the photons are always counted.

In the case of a fully coherent stationary photon field, the probability $p(n, \Delta t)$ of registering $n = 0, 1, 2, \dots$ photons within the preset time interval Δt is Poissonian for *all* values of M , while an ideal chaotic stationary field is subject to a geometrical distribution, but only in case of $M = 1$. With increasing M , $p(n, \Delta t)$ of the chaotic field approaches more and more closely the Poissonian distribution of the fully coherent field. Hence, the agreement of $p(n, \Delta t)$ with a Poissonian distribution is an indication of either a coherent or a high- M -value chaotic field. In order to elucidate this point further, we altered Δt , and the spectral band-width ΔM by using longpass filters, where $p(n, \Delta t)$ was calculated from the measured count rates of the subjects under investigation, in a quasi-stationary state. In 15 experiments with one thousand

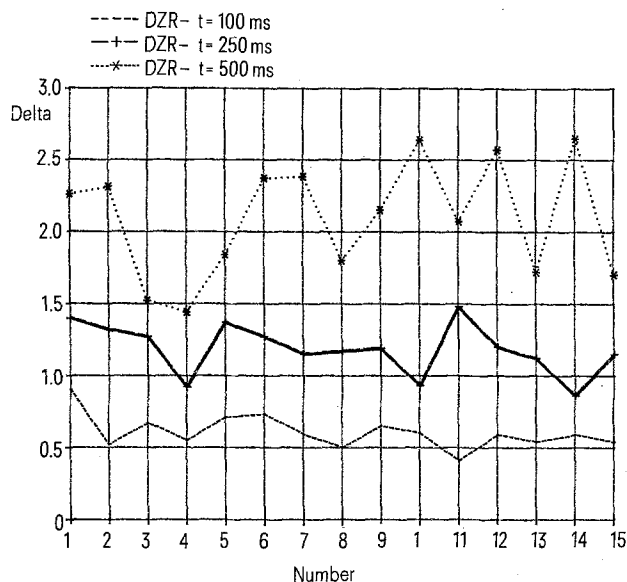


Figure 4a. For the dark count rate of the photon detector the expected deviation of its photocount statistics $p(n, \Delta t)$ from a Poissonian distribution (expressed in terms of the δ -value, see text) is observed: δ increases with increasing sampling time interval Δt . ($\delta(100 \text{ ms}) = 0.61 \pm 0.12$, $\delta(200 \text{ ms}) = 1.19 \pm 0.18$, $\delta(500 \text{ ms}) = 2.09 \pm 0.40$). This indicates the chaotic nature of the noise-source. Fig. 4a displays the δ -values of the 15 control experiments to figs 4b and 4c, based on 200 measuring values.

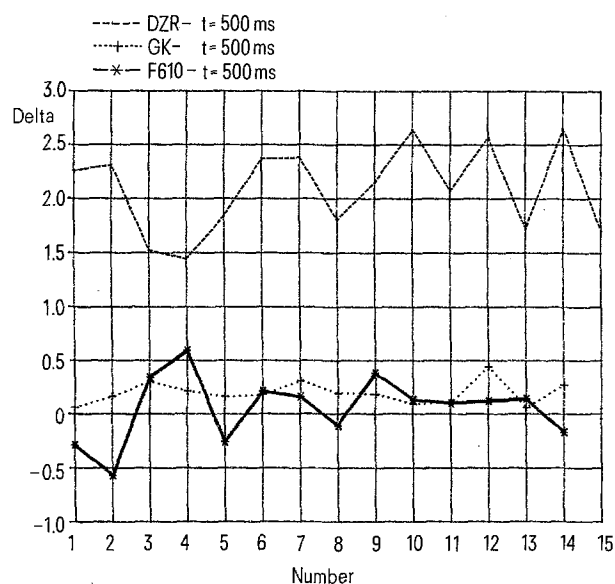


Figure 4b. Compared to the δ -values of the dark count rate ($\delta = 2.09 \pm 0.4$ for $\Delta t = 500 \text{ ms}$) the δ -values of biophoton emission from cucumber seedlings ($\dots + \dots$) are much lower ($\delta = 0.19 \pm 0.11$ for $\Delta t = 500 \text{ ms}$), indicating a much higher degree of coherence. If one limits the spectral bandwidth with the aid of a longpass-filter RG 610 (Schott-Mainz) one does not get, as expected for a chaotic field, a larger deviation of $p(n, \Delta t)$ from the Poissonian distribution. In contrast, the agreement seems to become even better ($\delta = 0.06 \pm 0.31$ for $\Delta t = 500 \text{ ms}$), thus indicating again a high degree of coherence.

measured values each, we compared $p(n, \Delta t)$ of the dark count rate with that of different samples of 7 day-old cucumber seedlings (*Cucumis sativus*). As a measure of agreement with the Poissonian distribution, one can take the value

$$\delta \equiv \frac{\sigma^2 - \langle n \rangle}{\langle n \rangle}$$

where $\langle n \rangle$ is the average count number within the preset time Δt , and σ^2 its variance.

Agreement with a Poissonian distribution is here expressed as $\delta = 0$, while $\delta > 0$ as a bunching effect indicates a chaotic source. $\delta < 0$ means here that antibunching takes place. As expected, the chaotic noise of the equipment gives rise to increasing δ with increasing Δt . This behavior is displayed in figure 4a. However, the biophoton emission shows just the opposite δ -dependence. Without filters, the mean value of δ is 0.19, while that of measurements performed with a longpass filter RG 610 (Schott, Mainz) turns out to be $\delta = 0.06$ (fig. 4b). In addition, the alteration of the measuring time interval Δt does not considerably change the δ -value (fig. 4c). Rather, one observes the tendency of decreasing δ with increasing Δt , leading in some cases to significant antibunching-effects (Nrs 1, 2, 5, 8, 14).

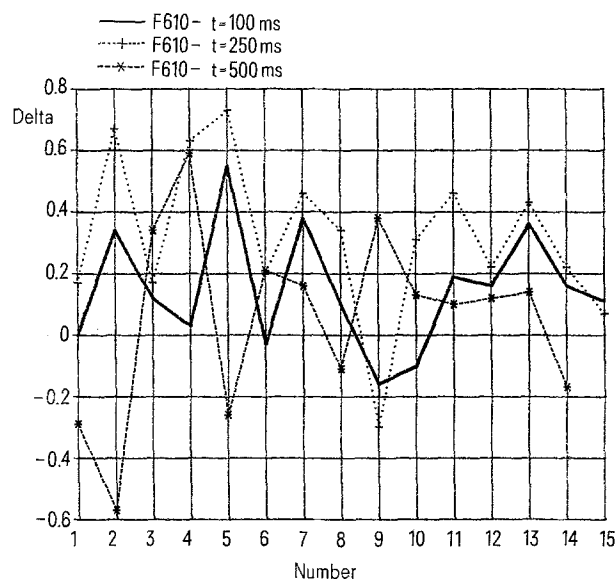


Figure 4c. In contrast to the dark-count rate of fig. 4a the biophoton emission – here from seedlings of *Cucumis sativus* – exhibits a tendency even to a lower δ -value with decreasing bandwidth and increasing Δt . Like in fig. 4a, always 2000 measurement values are subject of the calculation. The mean error, taking into account time-dependent variations of the equipment, is of the order 10%. Hence, even antibunching effects (see experiment Nr. 1, 2, 5, 8, 14) are likely or even evident. This supports the hypothesis that the coherence of biophotons (corresponding to $\delta = 0$) originates from a counterbalance of bunching ($\delta > 0$) and antibunching ($\delta < 0$) within the biological system.

Chaos and/or Order

An ideal chaotic system is a thermal equilibrium system, while the alternative, namely a well-ordered state, is represented by a fully coherent field.

Let us therefore imagine a system composed of matter and interacting photons, which is either a closed system at temperature T or, alternatively, represents an open system of coherent states.

The spectral as well as the total radiation intensity of an ideal chaotic system, corresponding to the 'black body radiation', is well known. It is the result of maximum entropy under the constraint that, by random absorption and reemission of photons from the interacting matter, the energy remains constant. Thus it represents a stationary state that is in thermal equilibrium with its environment. Actually, the radiation from electric bulbs, from the sun, or the infrared heat radiation from the human body are appropriate examples of black-body radiation at different temperatures T . Since the time intervals for counting 'ultra-weak' photon emission from living tissues are always many orders of magnitude longer than the time of thermal dissipation of a photon from condensed matter in thermal equilibrium, the quasi-stationariness of PE should be governed by just the same quasi-thermal equilibrium as the infrared heat radiation from living tissues.

However, this is by no means the case: figure 5 demonstrates that the spectral intensity of PE, and consequently the probability $f(\lambda)$ of occupying excited states of energy $\frac{hc}{\lambda}$, is by many, up to at least 40 orders of magnitude higher than that of thermal equilibrium radiation. In addition, in contrast to black-body emission $f(\lambda)$ exhibits

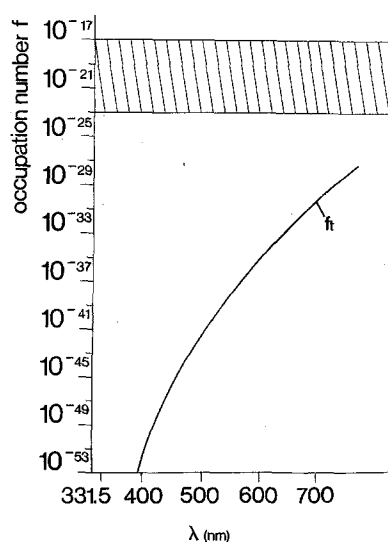


Figure 5. The probability f of occupying the (vacuum) phase space is for living systems completely different from that of a thermal equilibrium system (f_t , which follows a Boltzmann distribution). From the spectral intensity of 'low level luminescence' one calculates that f of living tissues lies 'far away from equilibrium' in the hatched zone, exhibiting (almost) no wavelength dependence ($f \approx \text{constant}$).

(almost) no wavelength-dependence, or $f(\lambda) \approx \text{constant}$. This rule $f(\lambda) \approx \text{constant}$ (fig. 5; see also references 39, 41, 46, 52) corresponds to a stationary state with almost the same conditions as those of thermal equilibrium, but exhibits one decisive change, namely the omission of the constraint of energy conservation. In other words; if a closed system in thermal equilibrium turns continuously into an open one, in which there is always enough (non-thermal) energy available, the Boltzmann law $f(\lambda) = \exp(-hc/kT)$ turns into $f(\lambda) = \text{constant}$.

This interesting link between a closed and an 'ideal' open system does not exclude the possibility that $f(\lambda) \approx \text{constant}$ is a casual consequence of a spontaneous chemiluminescence. However, it is a necessary but not sufficient condition of a phase-transition between a chaotic and an ordered regime in the optical range^{39-41, 46}.

In order to exclude the randomness of a rare spontaneous chemiluminescence, one might examine the temperature-response of PE. If we change the temperature T by a constant gradient $\frac{dT}{dt}$, we expect for the time-dependence of intensity $i(t)$ the relation

$$\left(\frac{\partial i}{\partial t}\right)_{\alpha, \beta, \dots} = \left(\frac{\partial i}{\partial T}\right)_{\alpha, \beta, \dots} \frac{dT}{dt} \quad (1)$$

where all possible parameters α, β, \dots are kept constant. This should be valid in particular for a spontaneous chemiluminescence, whose cross-section is simply a function of T .

However, instead of relation (1) we find an overshoot reaction (see fig. 6), which in general is typical for the temperature-dependence of physiological processes^{5, 48}. At the same time this type of non-linearity corresponds again to a phase-transition governed by the rule $f(\lambda) \approx \text{constant}$, as has been demonstrated in a recent paper⁵⁵ (see also next paragraph).

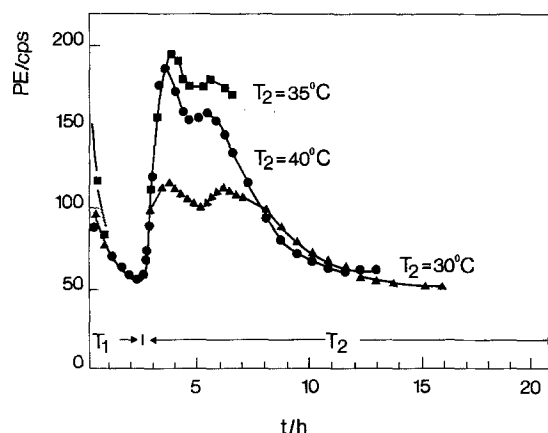


Figure 6. After adaption of cucumber seedlings to the dark chamber at a temperature $T_1 = 19^\circ\text{C}$, the temperature was increased to various temperatures T_2 within 1 h. Despite the constant T_2 , an overshoot reaction of photon emission is always observed. This characteristic dependence of PE is similar to that of various other physiological functions, indicating that 'biophotons' are either products or regulators of those processes.

The validity of (1) cannot, however, be completely excluded in the case that heat penetrates in just such a way that $\frac{dT}{dt} = f(t)$ as a possibly complicated function of time,

reflecting some delay of heat conduction. Then some transparency of the tissue for photons, originating from the interior parts of the system, should occur.

Consequently, the investigation of transparency becomes an important step in searching for the chaotic or coherent character of the luminescence.

Measurements of transparency of disperse media as well as of cell layers have yielded evidence that PE itself induces an extinction coefficient that is at least one order of magnitude lower than that for comparable artificial light (fig. 7)⁴⁵.

This non-linear optical absorbance, which is supported by the surprising, similar results of Mandoli and Briggs³¹, can again be traced back to a phase-transition with $f(\lambda) \approx \text{constant}$ ^{40, 45}, thus reflecting a high degree

of coherence^{56, 62}. Consequently, the hypothesis of chaotic luminescence cannot be sustained.

However, it remains unsatisfactory to present only indirect evidence of coherence. Interferometry, a powerful tool for studies in the usual range of light intensities, fails for photon emission from living systems, not only because of the low intensities involved, but also because of the broad spectral band belonging to a many-mode field (see fig. 5). The only suitable method is the use of photo-count statistics (PCS)^{2, 35}. It states that the probability $p(n, \Delta t)$ of counting n photons within a preset time interval Δt follows a geometrical distribution in the case of a completely chaotic stationary one-mode field, whereas in the case of a fully coherent stationary field the probability always follows a Poissonian distribution. For a multi-mode chaotic field the situation becomes more complicated, since, with an increasing number of modes, its $p(n, \Delta t)$ may approach more and more the same Poissonian distribution as that of a fully coherent field.

Because it is not possible to find a significant difference between the actually registered $p(n, \Delta t)$ and a Poissonian distribution^{41, 46}, either a coherent field or a chaotic field with at least M modes can be taken into consideration. We estimated the limit of M independent modes in a case where the PE was rather high and quasi-stationary, with the result $M \geq 10^5$ ^{41, 46}. This means that, within the range from about 200 to 800 nm, more than about 100,000 independent modes (with rather small line-widths) should contribute to PE, if it originates from a chaotic spontaneous luminescence. This possibility can actually not be excluded. However, it requires completely different interpretations from those involved in the case where a small number of possible biochemical reactions is considered. It has to be assigned to a very large multiplicity of allowed optical transitions which are independent of each other. Almost each count reflects its own individual reaction. This again would, however, not explain the temperature-dependence of PE or the extraordinary transparency of materials to PE.

In order to find direct evidence of coherence, one has to change to non-stationary PCS⁴⁶. The basic idea is the following: If a completely chaotic field is excited, it decays according to exponential relaxation-dynamics^{8, 16, 17, 46, 60}. This exponential characteristic comes from a semi-group law⁶⁰, which provides a permanent loss of the system's memory. Under just the same (ergodic) conditions, the exponential decay turns into a hyperbolic one, as soon as a chaotic field changes into a coherent one. This holds not only for classical, but also for quantum description^{27, 28, 46}.

To elucidate this important point, let us look at the simple equation (2), which for $\kappa = 0$ reflects the equality of potential energy $x\ddot{x}$ of an oscillator with amplitude $x(t)$ and its kinetic energy \dot{x}^2 .

$$\langle x\ddot{x} \rangle = (1 + \kappa) \langle \dot{x}^2 \rangle \quad (2)$$

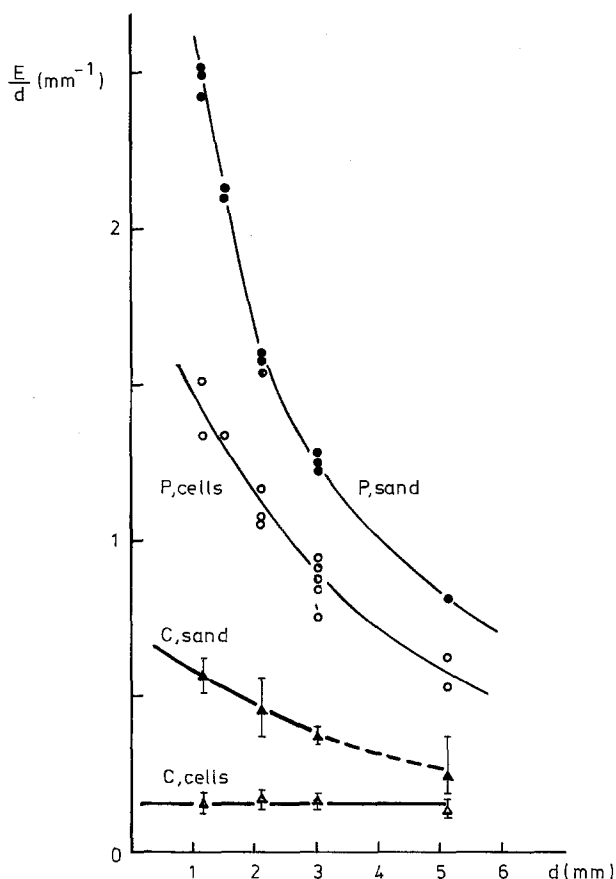


Figure 7. The extinction coefficient E/d (mm^{-1}) of sea sand (P, sand) and soya cells (P, cell) of various thickness d (mm) was first measured at $\lambda = 550$ nm in a Gilford 250 spectrophotometer, and then the E/d of photons emitted by cucumber seedlings, and passing through just the same layers of sand (C, sand) and cells (C, cells), respectively, was determined. It can be seen that 1) the transparency of both artificial and 'biological' light, increases with increasing thickness of the dispersive media, since E/d decreases with increasing d , and 2) the transparency to 'biophotons' is at least two orders of magnitude higher than that to artificial light (of comparable wavelengths).

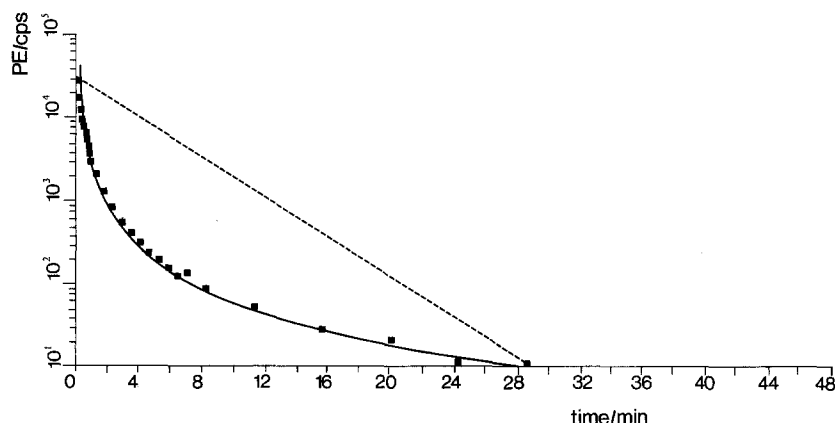


Figure 8. Instead of an exponential decay (dashed line), living cell populations (here tissue of *Bryophyllum daigremontanum*) exhibit a hyperbolic relaxation of photon intensity after exposure to white-light-illumination.

This holds for total as well as for spectral observation (here at $676 + 10$ nm). Under ergodic conditions, hyperbolic decay is a necessary and sufficient condition of coherent rescattering.

For $\kappa \neq 0$, we find a coherent restoring of kinetic energy as potential energy instead of chaotic rescattering under ergodic conditions.

The solution of (2) for $\kappa = 0$, i.e., $x = x_0 \exp(-t/\tau)$ with τ as relaxation time, turns into the hyperbolic law

$$x = x' = (t + t_0)^{-\frac{1}{\kappa}} \quad (3)$$

for $\kappa \neq 0$. Although this relation does not reflect any wavelength-dependence, we have to examine the relaxation dynamics of PE for total intensity as well as for spectral intensity, in order to avoid confusion with a possibly hyperbolic characteristic of the sum of many exponential decay-functions.

In almost all cases investigated so far a hyperbolic decay could be confirmed^{10, 41, 61}. Thereby it does not matter whether a total or a spectral measurement of PE after white-light or monochromatic illumination has been performed. An example, for which an interference filter of $\Delta\lambda \simeq 10$ nm was used, is displayed in figure 8. The experiments of Schamhart et al. and of Chwirot et al. indicate that κ is actually a measure of cooperativity and of coherence within the cell population^{10, 12, 61}. Changing

from white-light illumination to monochromatic excitation seems to change the real κ into a complex constant, giving rise to oscillations^{12, 41}.

It is worthwhile to note that a chaotic chemiluminescence should not react very sensitively to weak external influences, while a fully coherent field must react in principle to all perturbations, even of low amplitudes. Actually, rather high sensitivities can be registered, as is demonstrated for instance in figure 9. Hence, we can conclude that the hypothesis of a fully coherent field for PE reflects the reality rather better than the contrary hypothesis of a chaotic chemi-luminescence. Table 1 sets out all the opposing points.

Some essentials of a possible model

On a molecular level it is unlikely, if not impossible, that a coherent photon field originates from single uncoordinated luminescence events. Rather, experimental results^{11, 49} as well as some theoretical indications^{26, 28, 37, 38, 47} point to biopolymers, in particular exciplexes of DNA, as the essential source of a coherent

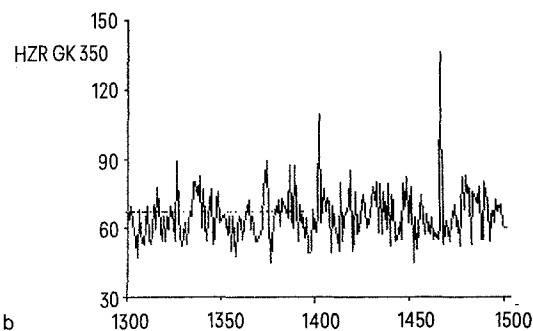
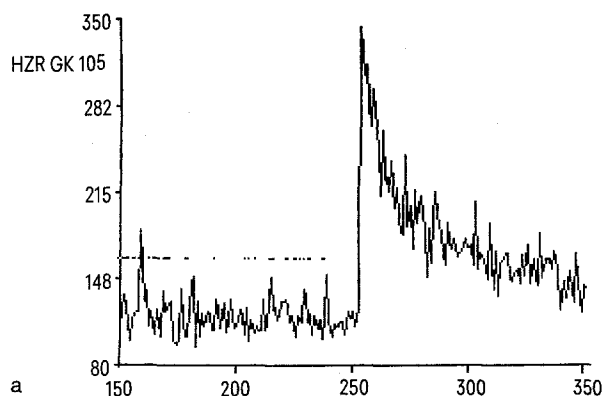


Figure 9. The biophoton emission (here in counts/s) during time (in s) can change significantly after addition of a poison (here diluted to a concentration of $1:10^5$ in physiological salt solution, added at 250 s). In

contrast, the addition of the solvent (at 1400 s), never changed the intensity distinctly.

Table 1. Expected properties of a chaotic (spontaneous) luminescence field versus an ideal coherent (regulatory) field. The experimental results are italicized, where experimental evidence has been provided.

Criterion	Chaotic field	Coherent field
Localization	'Spontaneous' chemiluminescence	Delocalized and factorizable electromagnetic field
Correlation to physiological or biological functions	'Imperfections' – no correlation –	<i>Correlation to many, if not all processes</i>
Temperature dependence	'Arrhenius'-plot (exponential kinetics)	Non-linear reactions (<i>overshoot-reactions, hysteresis-loops, etc.</i>)
Excitation-temperature	Near equilibrium (quasi black-body radiation)	<i>Far away from equilibrium</i> non-equilibrium-phase-transitions
Energy transport	Diffusion-controlled	Cooperation phenomena: <i>transparency</i> , but also protection (absorbance) possible
Sensitivity to external influences	Small	Possibly <i>high</i>
Photocount statistics for one mode	Geometrical distribution	<i>Poissonian distribution</i>
Spectral decay behavior under ergodic conditions	Exponential	<i>Hyperbolic</i>

electromagnetic field within living tissues. For a finite two-level system (which appears as the most simple approach), we obtain then consequently the balance equation

$$N_1 + 2 N_2 = N_0 \quad (4)$$

where N_1 and N_2 are the numbers of unexcited and excited exciplexes, respectively, and N_0 represents the total number of polymer units, e.g., base-pairs of DNA. The factor 2 accounts for the fact that always two molecular units, namely an excited and an unexcited one, form one excited exciplex (see, for instance, Birks⁴). Although it appears likely that the exciplex groundstate in biological matter far from equilibrium is subject to coherent vibronic and/or soliton interactions^{13, 15, 28, 29}, let us provide the most simple approach, namely a thermal dissipation. Hence, the groundstate kinetic energy is simply $N_1 \cdot kT$.

The excited state is subject to a chemical potential μ plus the energy C_1 that flows permanently to other units including cytoplasm etc. Consequently, we get for a stationary state the balance equation

$$N_1 kT + N_2 (\mu + C_1) = C_0 \cdot N_0 \quad (5)$$

where C_0 accounts for the total free energy per molecular unit. For the limit of thermal equilibrium we have for instance $\mu = 0$ and $C_0 = (1/2) C_1 = kT$.

Besides (4) and (5), Einstein's formula (6) is valid, where eq. (7) describes the radiation density within the system, and A , B are the Einstein coefficients of spontaneous and induced emission, respectively.

$$\dot{q} = \frac{hc}{\lambda} (AN_2 + (N_2 - N_1) q B) \quad (6)$$

$$q = \frac{A}{B} \left(\exp \left(\frac{C_2 - \mu}{KT} \right) - 1 \right)^{-1} \quad (7)$$

The energy hc/λ corresponds to the exciplex transition. Consequently we have also $C_2 = hc/\lambda$. Let us fix it here as a further parameter.

Since \dot{q} is a measure of the intensity of PE, the question becomes important whether stable regions at $\mu \neq 0$ occur besides of $\mu = 0$ and thermal equilibrium (with $\dot{q} = 0$). Figure 10 demonstrates that we actually obtain a zone of conditional as well of unconditional stabilities, which may work as the basis of biological evolution. At about

$f(\lambda) = \frac{N_2}{N_1} \simeq 1$ we obtain different branches of feedback-coupling, following equation (8), which is result of eqs. (4–7).

$$\dot{q} = \frac{\beta}{2 + \frac{1}{f}} \left(1 + \left(1 - \frac{1}{f} \right) \frac{1}{\exp(x) - 1} \right) \quad (8)$$

$$\text{where } \beta = \frac{hc}{\lambda} \cdot N_0 \cdot A$$

$$x = \frac{C_2 - \mu}{KT}$$

Table 2 displays all the possible cases of eq. (8) (see also figures 10 and 11).

We may now discuss the consequences of cases I and II. Ia corresponds to thermal equilibrium which obviously does not describe the real situation. Consequently we are concerned either with Ib and/or IIb, since the actual $\dot{q} > 0$ is much higher than that of equilibrium states.

Since μ is actually of the order $C_2 \simeq \frac{hc}{\lambda}$, we have to take into account case IIa, too.

This corresponds to a metabolic 'feeding' of excited states, either by photon transfer or chemical 'pumping'. Since in this region of $\mu \simeq C_2$ the PE-characteristics are sensitively dependent on overshoot or undershoot of μ as compared to C_2 and f versus 1, this region is subject to very sensitive feed-back coupling, which is conditionally stable. As has been shown in previous papers, photon storage, for instance, corresponding to the formation of excited exciplexes, lowers μ at the same time. Therefore we have to turn to case IIIb. Increased emission, on the other hand, lowers f in such a way that case IIa results,

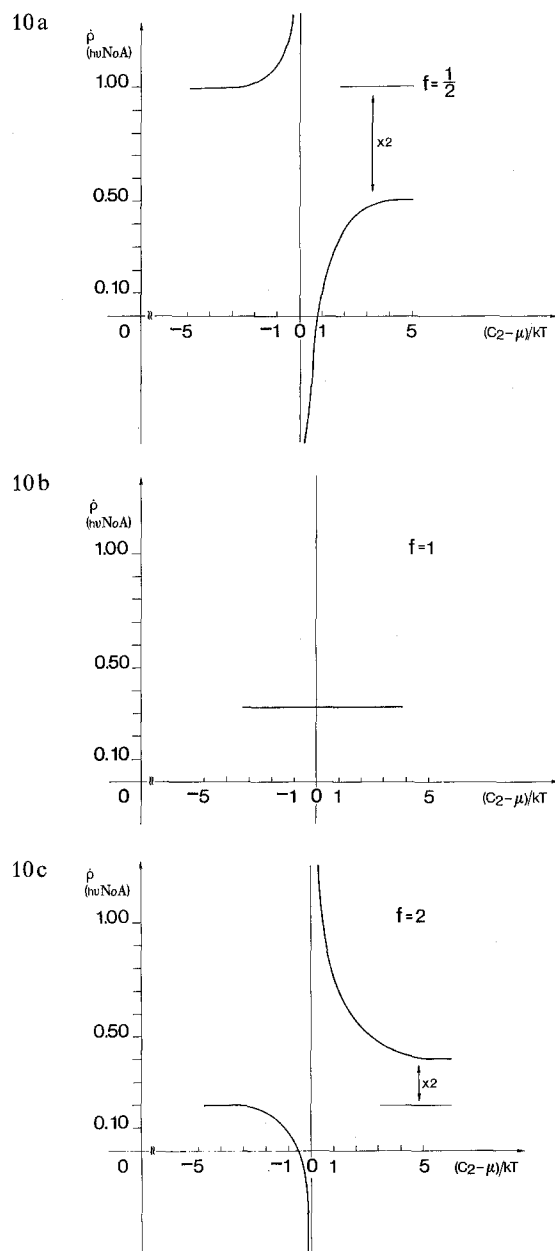


Figure 10. 'Far away' from thermal equilibrium there is a conditionally stable region of photon emission from exciplex-polymers at $f \approx 1$ and $C_2 \approx \mu$. The change of photon emission or photon trapping (storage) depends on μ . This dependence is displayed for values $f < 1$ ($f = 1/2$, fig. 10a), $f = 1$ (fig. 10b), and $f > 1$ ($f = 2$, fig. 10c). It demonstrates the stability discussed in the text and table 2.

which may return to Ib, IIIa, by pumping, or even IIIb, which would again result in IIa.

The time-dependence of eq. (6) can be taken into account by means of $q = \dot{q}\Delta t$, with Δt as a preset small time interval, and by coupling of eqs. (5) and (6). The solution is then uniquely determined after 1) specification of the initial values $f = N_2/N_1$ and q , 2) the determination of the parameter C_0/kT and 3) the iteration of these equations.

By use of this method which is very common now in the framework of the so-called 'deterministic chaos', one finds agreement with all the conclusions just drawn from

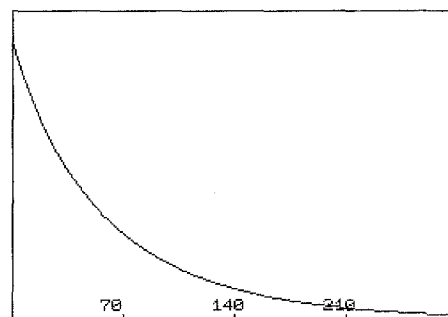


Figure 11a. The intensity of biophoton emission in the course of time (in arbitrary units) according to our thermodynamical model. As initial conditions are chosen:

$q = 1.1 \text{ A/B}$; $N_2/N_1 = 1.1$; $C_0/kT = 1.1$; $h\nu \cdot N_0 \cdot B \Delta t = 10^{-2}$. The intensity approaches a stable stationary state of final emission.

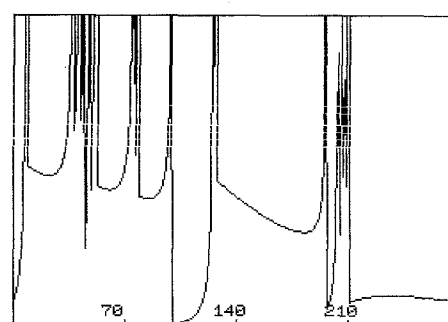


Figure 11b. The same as in fig. 11a with the only difference that at $t = 0$ for $C_0/kT = 0.99$ has been chosen. Now, the intensity fluctuates according to a chaotic regime.

Table 2

μ	f	\dot{q}	Case
≈ 0	$\ll 1$	$\rightarrow 0$	Ia quasi-thermal
	≈ 1	> 0	Ib quasi-coherent
$\leq C_2$	≈ 1	≤ 0	IIa pumping
	≈ 1	≥ 0	IIb coherent emission
$> C_2$	≈ 1	≤ 0	IIIa storage
	≈ 1	≥ 0	IIIb degradation
$\pm \infty$		> 0	IV quasi-crystalline

the stationary equations. In particular, regions of 'chaos' and 'order' can be distinguished. The figure 11 displays an example of a stable region, where the photon intensity after excitation runs into a stationary state with weak but final amplitude, and in comparison an example of an unstable state not far away from this stable one, where the same initial conditions but one have been chosen.

It is worthwhile to note that cases I and IV have to be included among the possible cycles of feedback-coupling, at least on a long-time scale. The region I there corresponds to the region of cell division (growth), while the case IV can be assigned to states of high differentiation. All these correspondences to biological functions have been discussed elsewhere^{34, 42-44}.

1 Adam, W., Biologisches Licht. Chemie in unserer Zeit 7 (1973) 182-191.

2 Arecchi, F. T., Photocount distribution and field statistics, in: Quantum Optics, pp. 57-110. Ed. R. J. Glauber. Academic Press, New York/London 1969.

- 0014-4754/88/070576-10\$1.50 + 0.20/0
© Birkhäuser Verlag Basel, 1988